Transformation, Green to Orange-Red, of a Porous Silicon Photoluminescent Surface in Solution

James L. Gole*

School of Physics, Georgia Institute of Technology, Atlanta, Georgia 30332-0430

David A. Dixon

Environmental Molecular Sciences Laboratory, Pacific Northwest National Laboratory, P.O. Box 999, K1-83, Richland, Washington 99352

Received: July 7, 1997; In Final Form: October 21, 1997[⊗]

The green and orange-red photoluminescent (PL) emissions characteristic of a porous silicon (PS) surface are excited with a variety of UV light sources and observed during and directly following the in situ (in solution) etching of a PS surface in a 20% HF in MeOH or 20% HF in H_2O solution. Experimental observations of the time dependent behavior of this in situ PL are combined with a quantum chemical modeling of the low-lying electronic states of the silanone-based silicon oxyhydrides to suggest that the initially observed and relatively long-lived green PL, its subsequent transformation to a final orange-red emission, and its stabilization in an ethylene glycol solution are to be associated with oxyhydride electronic transitions and the chemical transformation of surface-bound oxyhydrides.

Introduction

Electrochemically etched porous silicon wafers have attracted considerable attention due to their room-temperature visible light emission observed as photoluminescence (PL) upon excitation (PLE) with a variety of visible and ultraviolet light sources.[1−3] Under the appropriate in situ conditions, PS first displays a green luminescence[4,6] which would appear to be excited during the early and intermediate stages of the etching process. The photoinduced green luminescence then transforms to a final orange-red photoluminescence (600−800 nm), although the precursor emission which is excited on the PS surface can be stabilized for extended periods with appropriate solvation.[4,5] Here, we evaluate this green to orange-red transformation and its potential correlation with an oxidation cycle involving the silanone-based silicon oxyhydrides. We thus correlate the observations of this transformation under specific experimental conditions with detailed quantum chemical calculations to suggest a source of the luminescent sites.

The ultraviolet light induced luminescence from PS, which is strongly affected by the physical and electronic structure of the PS surface and by the nature of the etching solution used to produce the surface, is thought to emanate from regions at or near this surface. One popular hypothesis asserts that the PL results from the radiative recombination of quantum-confined electrons and holes in columnar structures or undulating wires.[6−10] A second explanation suggests the importance of surface localized states, involving irregularly shaped small crystallites that are not perfectly passivated, wherein elementary excitations are first trapped prior to recombination leading to the PL.[11,12] Yet a third explanation contends that the PL results from the presence of surface-confined molecular emitters. These include polysilane,[13] the complex siloxene ($Si_6O_3H_6$), and the compound that results as the highly symmetric siloxene is thermally "annealed".[14−16] Using the optical detection of magnetic resonance (ODMR), Stutzmann[14−16] and co-workers have clearly established that the PS "red" emission results from a triplet state (triplet exciton) which is thought to phosphoresce. Because of the close analogy of both the ODMR and optical excitation (PLE) and photoluminescence spectra of PS and "annealed" siloxene, Stutzmann et al.[14−16] suggested this molecule as the origin of the PS photoluminescence. While this prima facie evidence is enticing, we have noted that it may suggest a more general origin for the observed orange-red PL in the form of the functional groups and fluorophores which not only constitute the structure of "annealed" siloxene but in a more general sense are associated with the silicon oxyhydrides.[17] In fact, Steckl et al.[18] have obtained evidence for the presence of the silicon oxyhydrides in stain etched porous silicon thin films, correlating their observations with crystallinity and photoluminescence. Further, in a study of the thermal oxidation and nitrogen annealing of luminescent PS, Yan et al.[19] have obtained evidence that residual hydrogen exists in a 1000 °C/10 min thermally oxidized PS film in the form of SiOH. These studies refer to samples that have been removed from the HF etching solution; however, with the known substantial hydride coverage of the silicon surface during the etching process,[20] the subsequent oxidation of this surface to form silicon suboxide and silanol constituencies, and hence the oxyhydrides, is not surprising in either an in situ aqueous etch or ex situ environment.

We have carried out an extensive series of experiments[5,17,21,22] evaluating the in situ PL both during and following the etching process in both aqueous and nonaqueous etching solutions. These studies, coupled with quantum chemical calculations suggest that the nature of the PS green and orange-red photoluminescence correlates well with the silanone-based silicon oxyhydrides as they are bound in what might be termed defect sites[3] to the PS surface. Here, we present the results of

[⊗] Abstract published in *Advance ACS Abstracts,* December 1, 1997.

S1089-5647(97)02214-1 CCC: $15.00
Published on Web 01/01/1998

the first time dependent observations of the PL observed in an HF-based etching solution during the early stages of electrochemical etching and, following, in a stabilizing ethylene glycol solution. We then present the results of detailed quantum chemical modeling which suggest a close correlation between the calculated locations of the lowest lying silanone-based silicon oxyhydride triplet excited states and the observed green and orange-red PL emissions. In combining the results of these calculations on the oxyhydrides with experiment, we demonstrate that the changes in bonding associated with electronic transitions involving these species, especially in the SiO-related bonds, can provide a plausible and consistent explanation for the observed character of the PL emissions.

Experimental Section

The overall experimental configuration used to monitor laser or mercury lamp induced photoluminescence from porous silicon (PS) samples is discussed in detail elsewhere.[5,17] Briefly, porous silicon (PS) samples were prepared as a result of the anodic etching of (100) silicon wafers. Boron-doped p-type silicon from MEMC (Dallas, TX) with a resistivity of 2 Ω cm was used in the experiments, the results of which we outline in the present discussion. Electrical contact was made to the back of the silicon by first sputtering aluminum followed by the attachment of a metal wire using conductive paint. The PL from porous silicon was excited using a KrF laser at 248 nm or a nitrogen (N_2) laser at 337.1 nm. The PL was excited while the samples were still in the etching solution, in the early stages of the etching process, or after transfer to an ethylene glycol solution. In the process of transfer, the samples were first rinsed in ethylene glycol and then placed in a cuvette similar to that used in the etching process in which the etching solution was replaced by the glycol.

The PL was dispersed through a McPherson monochromator and detected with a Hamamatsu 446 phototube. The output of the phototube was sent to an SR400 (Stanford Research Series) photon counter controlled by an IBM PC which was also used to collect the data for further analysis. A typical scan, first from 490 to 730 nm, in 2.5 nm steps with 30−40 laser shots per data point for the excimer laser running at a repetition rate between 20 and 30 Hz, requires ∼3.5−4 min. This scan can be immediately taken in reverse, furnishing a valid internal check of the changes taking place during the scan cycle. Spectral calibration was accomplished with the individual laser excitation wavelengths, monitored in second order. The nature of the etching and, where appropriate, ethylene glycol solution used for a given experiment is indicated in the figure captions.

Quantum Chemical Calculations. We have been concerned with the evaluation of the low-lying electronic transitions of the silicon oxyhydrides and their potential role as the source of the luminescence from PS.[23−25] We have employed both ab initio molecular orbital theory and density functional theory (DFT-ground-state singlets) using the program systems DGauss[26] (DFT calculations) and Gaussian 94[27] (ab initio MO calculations) to model these compounds. The molecules $Si(O)H_2$, $Si(O)H(OH)$, $Si(O)(OH)_2$, $Si(O)H(OSiH_3)$, $Si(O)H(SiH_3)$, $Si(O)(OH)(SiH_3)$, and $Si(O)(SiH_3)_2$ have been tested as models for the types of sites that might be present on a hydrogen-passivated silicon surface[28] undergoing oxidation. Further calculations were carried out on the ground and lowest lying electronic states of the silylenes and the SiXYZ compounds, which vary through the series from SiH_3 to $Si(OH)_3$.[25] Although cluster models such as these do not include the long-range Coulomb effects present in the bulk, they can provide clear insights into the effect of changing the functional groups which might be attached at the silicon surface.

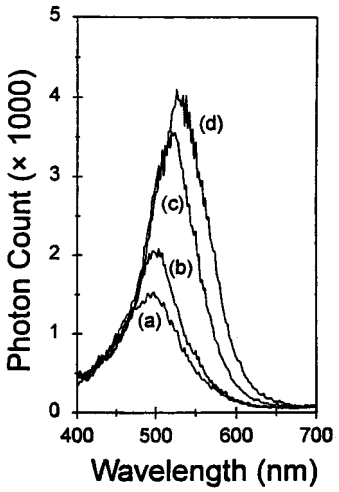

Figure 1. Photoluminescence spectra obtained in situ in the early stages of the etching process. The spectra were obtained from a 2 Ω cm wafer in a 20% HF in MeOH solution (MeOH @ 6 mol/L HF, ∼7 mol/L H_2O) using a KrF excimer laser for excitation as the gate includes the first 100 μs of emission. Spectrum a was obtained after an initial 4 min etch at 10 mA/cm^2, while spectra b, c, and d were obtained subsequently after additional 6 min etch cycles.

Optimized geometries were calculated at the DFT level for the ground-state singlet and in some cases for the lowest excited triplet state of the silanones using a polarized triple-ζ basis set.[29] Second-derivative calculations demonstrate that these structures represent minima.[30] These optimum geometries were then used in molecular orbital calculations at the MP2 level[31] with a polarized double-ζ basis set.[32] The lowest lying triplet excited states were subsequently evaluated. Geometries were reoptimized at the MP2/DZP level, and frequency calculations were done for these optimized geometries. To evaluate corrections to the ground-state singlet-low-lying-triplet separations determined at the MP2/DZP level, higher order correlation corrections were done on $Si(O)H_2$ at the optimized geometries. These calculations were done at the CCSD(T) level[33] with a triple-ζ basis set[34] augmented by two sets of polarization functions on all atoms and by f functions on the heavy atoms.

Results and Discussion

Experimental Observations. The green PL (∼520 nm)[4,5] which can be excited by a KrF laser on a PS surface during the early and intermediate stages of the etching process is considerably more pronounced after a silicon wafer has been treated in an aqueous etching cycle at moderate HF concentrations (20% HF in H_2O or MeOH).[5] Therefore the present considerations focus on these etches. If the polished silicon wafer is electrochemically etched in MeOH, the concentration of HF is 6 mol/L. The concentration of water in a 20% HF in MeOH solution is approximately 7 mol/L. The transformation from green to orange-red PL during the earliest stages of etching in this solution can be followed from an onset point at which the photoinduced emission is dominantly a deep green with tinges of orange and produces the spectra depicted in Figure 1, peaking first at ∼500 nm and subsequently shifting to a peak at ∼550 nm. From the spectral scans depicted in Figure 1, it should be apparent that the emission red shifts with time in the etching solution. Eventually, the PL will begin to decay at a rate that depends on the specific constituency of the etch solution.[5] If we simultaneously monitor the time dependent growth of the

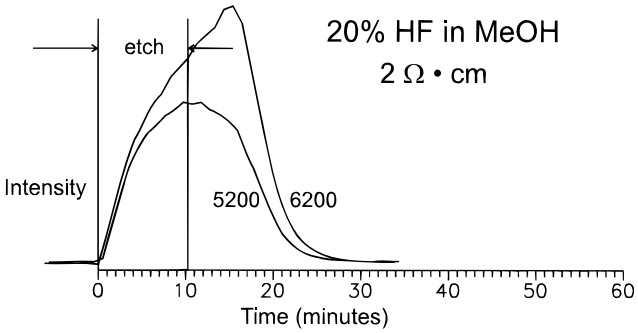

Figure 2. Plot of in situ photoluminescence (PL) intensity at 520 and 620 nm as a function of time after etching. The spectra were obtained from a 2 Ω cm wafer in a 20% HF in MeOH solution (MeOH @ 6 mol/L HF, ~7 mol/L H_2O) using a KrF excimer laser for excitation. The emission is monitored from the onset of the etch cycle, through the 10 min etch at 4 mA/cm^2, and subsequently to the point of complete decay of the PL.

emission at 520 and 620 nm,[5] for the $HF_{(aq)}$−MeOH etch solution, we find that the green and orange-red emissions, at least initially, appear to parallel each other and rise rapidly (Figure 2). These PL emissions are apparent with much less than 1 min of etching. Just after the etching current is terminated, the 620 nm PL at first increases, whereas the 520 nm emission intensity, which corresponds to the intermediate green emitter, has reached its peak. The green emitter thus appears to be more closely correlated with the formation of those hydrides known to be formed initially in the etching process on the PS surface. Of possibly more significance, the PL spectra displayed in Figure 1 suggest that the PL peak wavelength is red shifting and growing more intense with time. This result suggests the etch solution induced conversion of a surface-bound constituent which can be excited to produce the green PL emitter to the corresponding species whose photoexcitation produces the subsequent orange-red emission. The decay of the 520 and 620 nm emissions is apparent (Figure 2) as the etched PS sample remains in solution. The *rate of loss* of the 620 nm luminescence clearly exceeds that of the 520 nm luminescence.

As we demonstrate in Figure 3a,b, for those samples that have been prepared in an etching process in 20% HF in MeOH, the transformation cycle at intermediate times (>10 min in Figure 2) can be impeded if the etched sample is first rinsed in ethylene glycol and then placed in an ethylene glycol solution.[4,5] In fact the transformation of the green PL can be slowed for an extended period while the glycol is also stabilizing the 620 nm emission. Similarly, although the time dependence for the luminescence at 520 and 620 nm, as depicted in Figure 4 for a sample prepared by etching in a 20% HF in water etch solution, is somewhat different, the PL stabilization due to ethylene glycol is apparent as it impedes the decay of both the 620 and 520 nm emissions.[5]

The sources of the green and orange-red PL also appear to be distinct emitters which are selectively excited by the light sources used in these experiments. Upon its removal from the etching solution, before drying, a freshly etched sample coated with the etching solution or one that has been rinsed in methanol or ethylene glycol appears green under Hg lamp excitation but orange-red when excited by a KrF or ArF laser. After the PS sample matures in air for an extended period, its transformation to an orange-red emitter is complete and, at all illumination wavelengths, the emission is strongly dominated by an orange-red luminescence. This suggests that two electronic transitions involving two species have been excited. Further, this result suggests that a surface-bound species that can be excited to

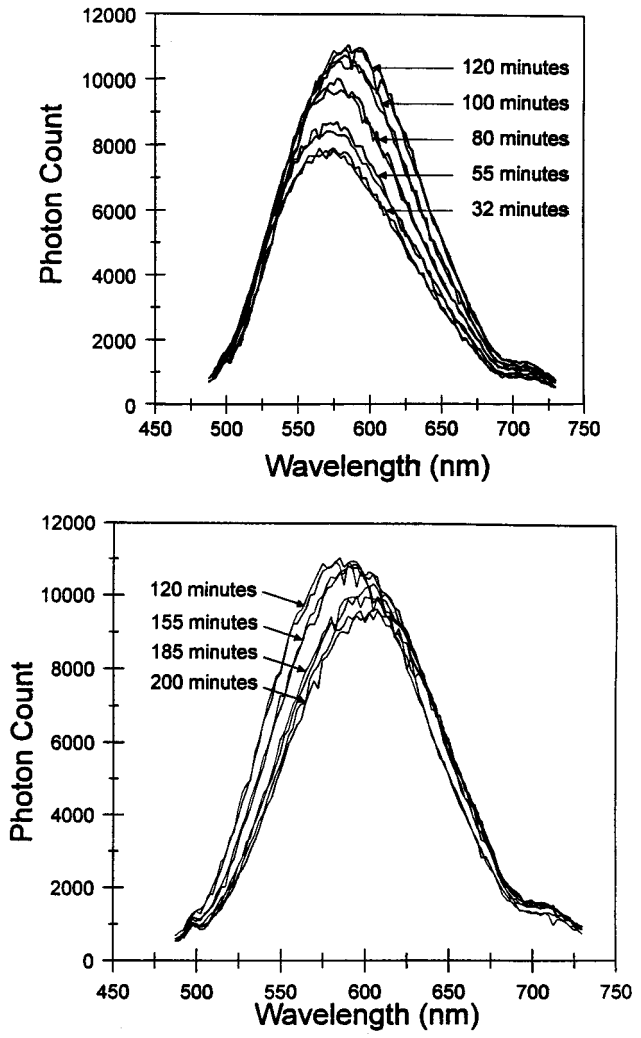

Figure 3. Photoluminescence (PL) spectra a and b obtained after an etched sample is placed in ethylene glycol solution. The porous silicon sample was obtained as a 2 Ω cm wafer was etched @ 10 mA/cm^2 for 4 min in a 20% HF in MeOH solution (MeOH @ 6 mol/L HF, ~7 mol/L H_2O). A KrF excimer laser was used for excitation as the gate includes the first 100 μs of excitation. Photoluminescence spectra were obtained for the indicated times after the sample was placed in the ethylene glycol solution by scanning first from the blue to the red and then immediately reversing the wavelength scan. The spectra first increase in intensity, showing a red shift from a peak at ~570 nm to ~595 nm. With increasing time, after ~120 min in the glycol solution, the PL continues to red shift (Figure 3b), to a peak wavelength at ~615 nm and slowly decreases in intensity.

produce the green emission represents an intermediate that has undergone a chemical transformation to that species that is optically pumped to produce the more frequently observed orange-red emission. Finally, we note that, for both the samples etched in 20% HF in MeOH and 20% HF in H_2O solutions, the decay of the light-induced PL can be followed visually at longer time to observe that the orange-red PL first decays away followed by the subsequent loss of any residual green PL emission. This behavior again suggests that the green emitter represents a distinctly different chemical intermediate whose chemical transformation would appear to be required for the formation of the orange-red emitter. While the rate of the "color" monitored transformation from the green to the orange-red emitter can be made to occur somewhat more rapidly in the presence of light from either the KrF or N_2 laser excitation sources,[5] the transformation, which can be monitored at intervals

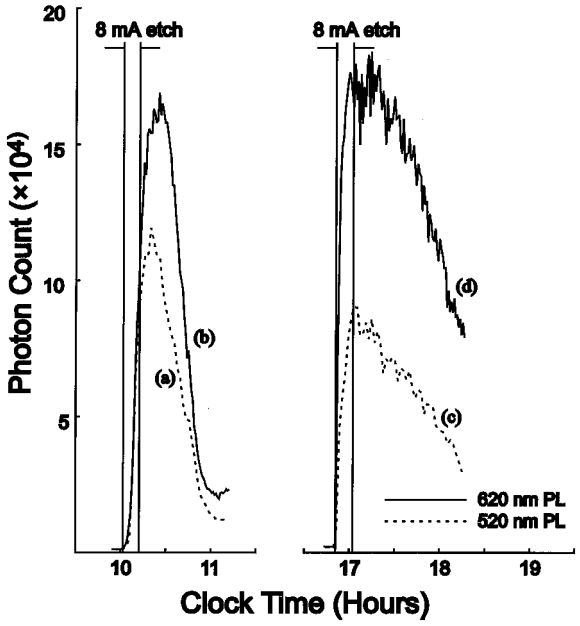

Figure 4. Plot of in situ photoluminescence (PL) intensity at (a) 520 and (b) 620 nm as a function of time after the onset of etching. The spectra were obtained from a 2 Ω cm wafer in a 20% HF in H_2O solution using an N_2 laser for excitation. Plot of in situ PL intensity at (c) 520 and (d) 620 nm as a function of time after the onset of etching where 500 μL of ethylene glycol is added to the etching solution (20% HF/H_2O). The emission in all scans is monitored from the onset of the etch cycle, through the 10 min etch at 4 mA/cm^2, and subsequently to the nearly complete decay of the PL. The introduction of ethylene glycol is seen to extend the period of PL, enhance the 620 nm PL relative to the 520 nm PL, and stabilize both the 520 and 620 nm emissions.

in a completely darkened room, is due overwhelmingly to a chemical effect which can be photochemically enhanced.

The green and orange-red emissions have been previously assigned to interlocking exciton fluorescence and phosphorescence emissions, respectively. The data in Figures 1−4, however, would suggest a chemical transformation process involving two distinct surface species whose optically pumped excited states have *comparable* emission lifetimes. Although the overlap of the features associated with the green and orange-red emitters prevents a ready evaluation of the radiative lifetime associated with the green emitter, its decay via radiative routes does not appear to be compatible with a fast fluorescence process and is clearly far less rapid than that of the short-lived SiO_2 emission at 450 nm.[35,36] Our observations suggest a chemical conversion between two moderately long-lived (several microseconds[15]) surface-bound constituencies and establish that an intersystem crossing process involving a short-lived green and long-lived orange-red emitter, as suggested by others,[4] seems far less likely.

Quantum Chemical Modeling. The most relevant results of our quantum chemical calculations are presented in Tables 1−3.[22] In Table 1, we summarize the SiO bond lengths calculated at the MP2/DZP level for the ground-state singlets and lowest lying excited-state triplets of several model silanone-based oxyhydride compounds that we have considered. Further calculations on the SiXYZ compounds from SiH_3 to $Si(OH)_3$[25] demonstrate that these molecules possess excited states whose lowest lying transitions all lie far into the ultraviolet region and are therefore not accessible to the light sources used in this study.

The calculations on the silanones demonstrate a significant change accompanying the transition to a low-lying excited triplet state which produces a considerable lengthening of the SiO bond.[26] As Table 2 indicates, for the appropriate silanones, accompanying changes in the Si−Si bond lengths are considerably smaller. Similarly, calculations on the corresponding silylene isomers indicate much smaller changes in the bond lengths and bond angles of their low-lying excited states which can be accessed via excitation spectroscopy in the appropriate spectral regions. The data in Table 3 indicate the calculated singlet−triplet separations for the model compounds of interest. It is noteworthy[17,25] that the calculated locations of the silanone-based silicon oxyhydride excited triplet states for Si(O)H(OH), $Si(O)(OH)_2$, $Si(O)H(OSiH_3)$, and $Si(O)OH(SiH_3)$, containing an OH or $OSiH_3$ moiety, and the known peak wavelength of the porous silicon (PLE) excitation spectrum (∼350 nm)[37] bear a clear resemblance to the known singlet−triplet splittings of the low-lying silicon monoxide intercombination band systems.[38] The large change in the SiO bond lengths indicated in Table 1 for all of the silanones, in turn, produces a large shift in the excited-state potentials relative to the ground state. The relative location of the ground- and excited-state potentials especially for the OH- or $OSiH_3$-bonded silanones will promote optical pumping high up the excited-state potential and a significant difference in the peak of the PLE excitation spectrum (∼350 nm) and the observed PL emission range (∼600−800 nm (orange-red) (see Figure 5)). While the data are consistent with a most efficient excitation pumping high up the excited triplet state manifold for these silanone-based compounds, it is also clear that there will be subsequent rapid nonradiative vibrational relaxation through the excited triplet manifold before the emission[17,25] of radiation.

There are additional striking aspects to the data in Tables 1 and 3. First, from Table 1 we note that whenever an OH or $OSiH_3(OR)$ group is bound to the silicon−oxygen bond, the

TABLE 1: Si═O Bond Lengths (Å) for Silanones at the MP2/DZP Level

molecule	r(SiO) singlet	r(SiO) triplet	Δr(SiO)
$Si(O)H_2$	1.545	1.700[a]	0.155
$Si(O)H(OH)$[b]	1.537	1.709	0.172
$Si(O)(OH)_2$	1.538	1.709	0.173
$Si(O)H(OSiH_3)$	1.537	1.708	0.171
$Si(O)H(SiH_3)$	1.553	1.695	0.142
$Si(O)(OH)(SiH_3)$	1.543	1.712	0.169
$Si(O)(SiH_3)_2$	1.560	1.681	0.121

[a] Bond length for the excited singlet is 1.705 Å. [b] Bond lengths for OH−Si−OH silylene are 1.670 Å for the ground-state singlet and 1.680 Å for the excited triplet.

TABLE 2: Si−Si Bond Lengths (Å) for Silanones at the MP2/DZP Level

molecule	r(Si−Si) singlet	r(Si−Si) triplet	Δr(Si−Si)
$Si(O)H(SiH_3)$	2.354	2.361	0.007
$Si(O)OH(SiH_3)$	2.342	2.365	0.023
$Si(O)(SiH_3)_2$	2.366	2.363	−0.003

TABLE 3: Ground-State Singlet−Excited Triplet Energy Separations for Silanones

molecule	ΔE(S−T) (kcal/mol)	ΔE(S−T) (eV)	$\sim\lambda_{Adiabatic}$ (nm)
$Si(O)H_2$	60.1	2.61	475
Si(O)H(OH)	70.9	3.07	403
$Si(O)(OH)_2$	71	3.08	402
$Si(O)H(OSiH_3)$	70.3	3.05	406
$Si(O)(OH)(SiH_3)$	71.2	3.09	401
$Si(O)H(SiH_3)$	57.3	2.48	499
$Si(O)(SiH_3)_2$	53.9	2.34	530
HSiOH	38.4	1.66	744
HOSiOH	64.2	2.78	445
SiH_3OSiOH	67.3	2.92	425

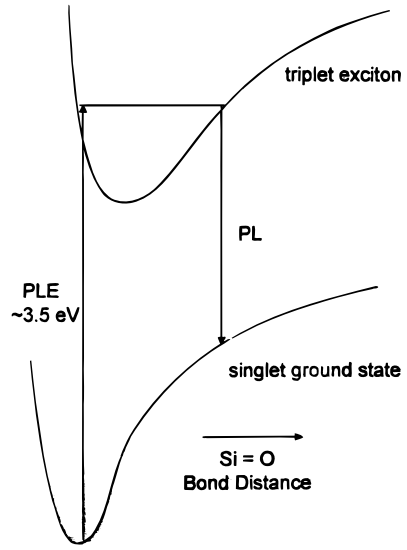

Figure 5. Rough schematic of silicon oxyhydride ground-state singlet and excited-state triplet potentials indicating the origin of the substantial difference in photoluminescence excitation (PLE) and subsequent photoluminescence (PL) emission energies.

calculated change, Δr(SiO), in transition is consistently a substantial 0.17 Å. Further, an additional OH group does little to affect this differential change in the bond length accompanying the singlet−triplet transition. In the absence of an −OH or −OR group, this change is notably smaller, decreasing from 0.155 Å for $Si(O)H_2$ to 0.121 Å for $Si(O)(SiH_3)_2$. These are distinct differences associated with −OR versus −R group bonding to the silicon which can have a considerable affect on the relative energies of PLE excitation and PL emission spectra. Further, we note the very similar adiabatic energy differences ($\Delta E \approx 3.05$ eV) that characterize those singlet−triplet transitions where an −OH or −OR group is bound to the silicon oxide bond. The shift of the excited triplet state relative to the ground-state singlet suggests that the maximum at ∼3.5 eV for the PLE excitation spectrum is quite consistent with a silanone-based oxyhydride containing an −OH or −OR group. Again, contrast the virtually identical energy increments for those silanones containing an −OR group to the much lower required pumping energies associated with the series $Si(O)H_2$ (0.155), $Si(O)H(SiH_3)$ (0.142), and $Si(O)(SiH_3)_2$ (0.121). Here, however, the indicated smaller change, Δr(SiO), in the SiO bond length is expected to lead to a considerably smaller red shift of the PL emission feature relative to the PLE excitation wavelength.

The results of the outlined quantum chemical modeling suggest that the unsaturated silanones with bound −OR ligands will produce a much larger red shift of the PL emission spectrum relative to the peak of the PLE excitation spectrum than those fluorophores having only −R group ligand binding. These latter silanones should be more efficiently excited at longer wavelengths, consistent with the experimental observations for Hg lamp vs KrF and ArF optical pumping. Further, the *unsaturated bonding* is necessary in order that the electronic transitions of interest for these Si, O, H compounds fall within the visible and ultraviolet regions. We suggest that the magnitudes of the calculated changes appear relevant to the correlation of the mechanism for PS formation with the assignment of the transforming green and final orange-red emissions[25] to the triplet excited state silanones in various stages of oxidation as R group ligands are converted to OR groups. Note that this assignment is also consistent with a somewhat enhanced transformation process induced by photochemistry, as it is likely that the long-lived excited triplet state which is produced and subsequently undergoes chemical transformation more rapidly in the presence of light.

TABLE 4: Select Calculated Dominant Vibrational Frequencies for Silanones[a]

molecule	vibrational frequencies (cm^{-1})	assignment
Si(O)H(OH)	1244	Si═O stretch
	869−896[b]	Si−O stretch + H−Si−O bend + H−O−Si bend
$Si(O)H(SiH_3)$	1150−1178[b]	Si═O stretch
	869[c]	SiH_3 bend + H−Si−Si bend
$Si(O)(SiH_3)_2$	1125−1165[b]	Si═O stretch
	898[c]	SiH_3 bend
$Si(O)(OH)(SiH_3)$	1222−1224[b]	Si═O stretch
	886[c]	SiH_3 bend + H−O−Si bend
$Si(O)H(OSiH_3)$	1245−1247[b]	Si═O stretch
	905	H−Si═O bend

[a] For a more detailed discussion see ref 25. [b] Range for DZP/MP2 and DFT/TZVP calculations (ref 25). [c] DZP/MP2 calculation of potential (ref 25).

The assignment of the green and orange-red emissions to the silanone based oxyhydrides in various stages of oxidation is also consistent with other experimental observations. The consistent growth of the PL with time during and for some period after the etch cycle suggests an increasing surface coverage of the PL emitters as their formation competes with dissolution. In the absence of an etching current, silicon dioxide and suboxide species formed during reaction are dissolved by the HF solution. The HF solution reacts with the silicon−oxygen bonds to dissolve SiO_x compounds while any silicon constituences formed on the surface during the initial etching process and terminated with hydrogen should remain untouched by the etching solution. This is certainly consistent with the cycle of growth and decay that we observe in these experiments.[5,17,21] As the oxide dissolution occurs as the PL decays in time, the oxidized silanone-based silicon oxyhydrides terminated with −OH or −OR groups that give rise to the orange-red PL emission would be expected to undergo dissolution at a more rapid rate than those −H or −R group terminated oxyhydrides that give rise to the green emission. This follows the decay cycle observed in the present experiments.

The outlined combination of experimental and quantum chemical results, that suggest that silanone-like fluorophores (Tables 1, 3) are to be associated with the PS green and orange-red PL emitters, would appear to correlate well with the IR spectra recorded by Dubin et al.[39] during the activation period for an electroluminescence that correlates with the observed photoluminescence. These authors *first monitor* the formation of silicon oxide. With increasing anodization they find that the SiH_x ($x = 1-3$) bands, as they are observed in the 2100 cm^{-1} region, decrease while O_ySiH_x bands in the 2150−2300 cm^{-1} region and assigned ν(SiOSi) features[40] in the 1050−1250 cm^{-1} range grow. This is consistent with the process of oxidative transformation from a green (e.g. analog of $Si(O)H(SiH_3)$) to orange red (e.g. $Si(O)H(OSiH_3)$ or $Si(O)SiH_3(OH)$) emitter.

Complete calculated infrared spectral frequencies for the silanones considered in Table 4 are discussed in detail elsewhere;[25] however, within the present context, it is appropriate to observe that at least two common and dominant frequency ranges are apparent. As cataloged and assigned in Table 4, these frequencies are consistent with the experimental observations of Dubin et al.,[39] the FTIR spectra obtained by Xie et al.[11] for PS films both freshly prepared and aged in air, and the observed FTIR spectra obtained by Hory et al.[41] and Mawhinney et al.[40,42]

in their monitoring of PS passivation and oxidation during posttreatments which include anodic oxidation. Further, the calculated ν(Si═O) stretch frequencies for silanoic acid and silicic acid given in Table 4 are in excellent agreement with the frequencies determined by Withnall and Andrews[43] (1249 cm^{-1} Si(O)H(OH) and 1270 cm^{-1} $Si(O)(OH)_2$) in solid argon matrixes. Si═O bonds on the PS surface may well be formed by the concerted reaction of a silicon surface atom and H_2O (with H_2 evolution).[44] Further, a similar concerted insertion into a Si−Si surface bond could lead to the formation of the Si−O−Si skeleton. In all of the observations reported,[11,39−43] a clear indication of oxide formation followed by the oxidation of SiH_x bonds is obtained. The studies of Mawhinney et al.[41] also clearly establish the formation of the Si−OH bond.

All of the infrared studies would seem to indicate an oxidation signaling SiO stretch region[25,43] and the development of a feature in the 870−890 cm^{-1} range. As Table 4 indicates, the assigned Si═O stretch region extends from 1125 to 1244 cm^{-1}.[42,43] All of the silanones considered in Table 4 also display a dominant 870−900 cm^{-1} mode which, in the presence of an OH or $OSiH_3$ ligand, appears to be associated with a combined Si═O stretch + H−Si−O (H−O−Si) bend, consistent with the observations of several workers.[11,18,41,42] However, we must note that Zacharias et al.[45] have studied the behavior of the 880 cm^{-1} band in hydrogenated amorphous silicon suboxide alloys, finding a minimal dependence on deuteration and therefore ascribing the feature to a non-hydrogen-related origin. Mawhinney et al.[42] have, however, provided a logical reason for this minimal shift. The assignment of this mixed mode feature is complex.

Summary and Conclusion

The results which we outline when correlated with experimental observation are consistent with the association of the green emitter with an intermediate surface-bound silanone where an Si═O group formed in the oxidation of the silicon surface is coupled to hydrogen or an adjoining SiH_x group. The resulting fluorophore might then be transformed to the orange-red emitter via an oxidative insertion into one or more Si−H (→ SiOH) or Si−SiH_x ($SiOSiH_x$) bonds. Hence, oxidative reactions on a porous silicon surface as they form and transform the silanone-based silicon oxyhydrides can account for the nature of the PL excitation spectrum and the observed distinct PL emission spectra in the green and orange-red spectral regions. We suggest that further studies whose aim will be to establish in situ direct probes of the oxyhydrides will represent an important contribution to the clear understanding of the photoluminescence from porous silicon, and we encourage these efforts.

Acknowledgment. We acknowledge helpful discussions with Mr. Frank Dudel. We also acknowledge financial support from the Office of the President at Georgia Institute of Technology under the auspices of the Focused Research Program. The quantum chemical calculations were performed under the auspices of the Office of Basic Energy Sciences, U.S. Department of Energy, under Contract DE-AC06-76RLO 1830 with Battelle Memorial Institute, which operates the Pacific Northwest Laboratory.

References and Notes

(1) Canham, L. T. *Appl. Phys. Lett.* **1990**, *57*, 1046.

(2) (a) Kanemitsu, Y. *Phys. Rep.* **1995**, *263*, 1−92. (b) John, G. C.; Singh, V. A. **1995**, *263*, 93−152.

(3) Prokes, S. M. *J. Mater. Res.* **1996**, *11*, 305.

(4) Astrova, E. S.; Belov, S. V.; Lebedev, A. A.; Rermenjuk, A. D.; Yu Rud, V. *Thin Solid Films* **1995**, *255*, 196−199.

(5) Gole, J. L.; Dudel, F.; Seals, L.; Bottomley, L.; Reiger, M. *J. Electrochem. Soc.*, submitted.

(6) See, for example: Calcott, P. D. J.; Nash, K. J.; Canham, L. T.; Kane, M. J.; Brumhead, D. *J. Phys. Condens. Matter* **1993**, *5*, L91−98.

(7) Calcott, P. D. J.; Nash, K. J.; Canham, L. T.; Kane, M. J.; Brumhead, D. *J. Lumin.* **1993**, *57*, 257.

(8) Nash, K. J.; Calcott, P. D. J.; Canham, L. T.; Needs, R. *J. Phys. Rev. B* **1995**, *51*, 17698.

(9) Cullis, A. G.; Canham, L. T.; Calcott, P. D. *J. Appl. Phys.* **1997**, *82*, 909.

(10) (a) Schuppler, S.; Friedman, S. L.; Marcus, M. A.; Adler, D. L.; Xie, Y. H.; Ross, F. M.; Chabal, Y. J.; Harris, T. D.; Brus, L. E.; Brown, W. L.; Chaban, E. E.; Szajowski, P. F.; Christman, S. B.; Citrin, P. H. *Phys. Rev. B* **1995**, *52*, 4910. (b) Schuppler, S.; Friedman, S. L.; Marcus, M. A.; Adler, D. L.; Xie, Y. H.; Ross, F. M.; Harris, T. D.; Brown, W. L.; Chabal, Y. J.; Brus, L. E.; Citrin, P. H. *Phys. Rev. Lett.* **1994**, *72*, 2748.

(11) Xie, Y. H.; Wilson, W. L.; Ross, F. M.; Mucha, J. A.; Fitzgerald, E. A.; Macauley, J. M.; Harris, T. D. *J. Appl. Phys.* **1992**, *71*, 2403.

(12) (a) Koch, F.; Petrova-Koch, V.; Muschik, T.; Nikolov, A.; Gavrilenko, V. *Mater. Res. Soc. Symp. Proc.* **1993**, *283*, 197. (b) Koch, F.; Petrova-Koch, V.; Muschik, T. *J. Lumin.* **1993**, *57*, 271. (c) Koch, F. *Mater. Res. Soc. Symp. Proc.* **1993**, *298*, 222.

(13) (a) Prokes, S.; Glembocki, O. J.; Bermudez, V. M.; Kaplan, R.; Friedersdorf, L. E.; Pearson, P. C. *Phys. Rev. B* **1992**, *45*, 13788. (b) Prokes, S. M. *J. Appl. Phys.* **1993**, *73*, 407.

(14) Fuchs, H. D.; Rosenbauer, M.; Brandt, M. S.; Ernst, S.; Finkbeiner, S.; Stutzmann, M.; Syassen, K.; Weber, J.; Queisser, H. J.; Cardona, M. *Mater. Res. Soc. Proc.* **1993**, *283*, 203.

(15) Stutzmann, M.; Brandt, M. S.; Rosenbauer, M.; Fuchs, H. D.; Finkbeiner, S.; Weber, J.; Deak, P. *J. Lumin.* **1993**, *57*, 321.

(16) Brandt, M. S.; Stutzmann, M. *Solid State Commun.* **1995**, *93*, 473.

(17) Gole, J. L.; Dudel, F.; Grantier, D. R.; Dixon, D. A. *Phys. Rev. B* **1997**, *36*, 2137.

(18) Steckl, A. J.; Xu, J.; Mogul, H. C.; Prokes, S. M. *J. Electrochem. Soc.* **1995**, *142*, L69−71.

(19) Yan, J.; Shih, S.; Jung, K. H.; Kwong, D. L.; Kovar, M.; White, J. M.; Gnade, B. E.; Magel, L. *Appl. Phys. Lett.* **1994**, *64*, 1374.

(20) Ubara, H.; Imura, T.; Hiracki, A. *Solid State Commun.* **1984**, *50*, 673.

(21) Dudel, F.; Gole, J. L.; Reiger, M.; Kohl, P.; Pickering, J.; Bottomley, L. *J. Electrochem. Soc.* **1996**, *143*, L164−166.

(22) Dudel, F. P.; Gole, J. L. *J. Appl. Phys.* **1997**, *82*, 802.

(23) Glinski, R. J.; Gole, J. L.; Dixon, D. A. *J. Am. Chem. Soc.* **1985**, *107*, 5891.

(24) Dixon, D. A.; Gole, J. L. *Chem. Phys. Lett.* **1986**, *125*, 179.

(25) Gole, J. L.; Dixon, D. A. *Phys. Rev. B*, in press.

(26) (a) Andzelm, J.; Wimmer, E.; Salahub, D. R. In *The Challenge of d and f Electrons: Theory and Computation*; Salahub, D. R., Zerner, M. C., Eds.; ACS Symposium Series No. 394; American Chemical Society: Washington, DC, 1989; p 228. (b) Andzelm, J. In *Density Functional Theory in Chemistry*; Labanowski, J., Andzelm, J., Eds.; Springer-Verlag: New York, 1991; p 155. (c) Andzelm, J. W.; Wimmer, E. *J. Chem. Phys.* **1992**, *96*, 1280.

(27) Frisch, M. J.; Trucks, G. W.; Schlegel, H. B.; Gill, P. M. W.; Johnson, B. G.; Robb, M. A.; Cheeseman, J. R.; Keith, T.; Petersson, G. A.; Montgomery, J. A.; Raghavachari, K.; Al-Laham, M. A.; Zakrzewski, V. G.; Oritz, J. V.; Foresman, J. B.; Closlowski, J.; Stefanov, B. B.; Nanayakkara, A.; Challacombe, M.; Peng, C. Y.; Ayala, P. Y.; Chen, W.; Wong, M. W.; Andres, J. L.; Replogle, E. S.; Gomperts, R.; Martin, R. L.; Fox, D. J.; Binkley, J. S.; Defrees, D. J.; Baker, J.; Stewart, J. P.; Head-Gordon, M.; Gonzales, C.; Pople, J. A. *Gaussian 94*, Revision B.2; Gaussian, Inc., Pittsburgh, PA, 1995.

(28) Prokes, S. M. *Electrochemical Society Interface*, Summer 1994; pp 41−43.

(29) Godbout, N.; Salahub, D. R.; Andzelm, J.; Wimmer, E. *Can. J. Chem.* **1992**, *70*, 560.

(30) Komornicki, A.; Fitzgerald, G. *J. Phys. Chem.* **1993**, *98*, 1398, and references therein.

(31) (a) Moller, C.; Plesset, M. S. *Phys. Rev.* **1934**, *46*, 618. (b) Pople, J. A.; J. S. Binkely Seeger, R. *Int. J. Quantum Chem. Symp.* **1976**, *10*, 1.

(32) Dunning, T. H.; Hay, P. J., Jr. In *Methods of Electronic Structure Theory*; Schaefer, H. F., III, Ed.; Plenum Press: New York, 1977; Chapter 1, McLean, A. D.; Chandler, G. S. *J. Chem. Phys.* **1980**, *72*, 5639.

(33) (a) Bartlett, R. J. *J. Phys. Chem.* **1989**, *93*, 1697. (b) Kucharski, S. A.; Bartlett, R. J. *Adv. Quantum Chem.* **1986**, *18*, 281. (c) Bartlett, R. J.; Stanton, J. F. In *Reviews of Computational Chemistry, Vol. V*; Lipkowitz, K. B., Boyd, D. B., Eds.; VCH Publishers: New York, 1995; Chapter 2, p 65.

(34) For the Si basis see: Dobbs, K. D.; Dixon, D. A. *J. Phys. Chem.* **1994**, *98*, 5290. For O and H, see: Dobbs, K. D.; Dixon, D. A.; Kormonicki, A. *J. Chem. Phys.* **1993**, *98*, 8852.

(35) See for example: Kontkiewicz, A. J.; Kontkiewicz, A. M.; Siejka, J.; Sen, S.; Nowak, G.; Hoff, A. M.; Sakthiviel, P.; Ahmed, K.; Mukherjee, P.; Witanachchi, S.; Lagowski, J. *Appl. Phys. Lett.* **1994**, *65*, 1436.

(36) The evaluation of a radiative lifetime for the green emitting precursor state can be complicated both by its continual formation and by its chemical transformation during the course of an emission decay measurement.

(37) See, for example: Brus, L. E.; Szajowski, P. F.; Wilson, W. L.; Harris, T. D.; Schuppler, S.; Citrin, P. H. *J. Am. Chem. Soc.* **1995**, *117*, 2915.

(38) See, for example: Green, G. J.; Gole, J. L. *Chem. Phys.* **1985**, *100*, 133.

(39) Dubin, V. M.; Ozanam, F.; Chazalviel, J. N. *Thin Solid Films* **1995**, *255*, 87−91.

(40) James Gole, L.; Dixon, D. A. *J. Phys. Chem.* **1997**, *101*, 8098.

(41) Hory, M. A.; Herino, R.; Ligeon, M.; Muller, F.; Gaspard, F.; Mihalcescu, I.; Vial, J. C. *Thin Solid Films* **1995**, *255*, 200.

(42) Mawhinney, D. B.; Glass, J. A., Jr.; Yates, J. T., Jr. *J. Phys. Chem. B* **1977**, *101*, 1202.

(43) Withnall, R.; Andrews, L. *J. Phys. Chem.* **1985**, *89*, 3261.

(44) See for example: Oblath, S. B.; Gole, J. L. *J. Chem. Phys.* **1979**, *70*, 581. Oblath, S. B.; Gole, J. L. *Combust. Flame* **1980**, *37*, 293. Meier, P. F.; Hauge, R. H.; Margrave, J. L. *J. Am. Chem. Soc.* **1978**, *100*, 2108. Hauge, R. H.; Meier, P. F.; Margrave, J. L. *Ber. Bunsen-Ges. Phys. Chem.* **1978**, *82*, 102.

(45) Zacharias; Dimova-Malinouska, D.; Stutzmann, M. *Philos. Mag. B* **1996**, *73*, 799.